Fabrication, Characterization, and Signal Processing Optimization of Flexible and Wearable Piezoelectric Tactile Sensors

V. Carluccio, L. Fachechi, V. M. Mastronardi, L. Natta, L. Algieri, G. de Marzo, F. Rizzi, and M. De Vittorio, *Senior Member, IEEE*

***Abstract*—Piezoelectric microelectromechanical systems (MEMSs) meet the growing demand for sensors with small sizes and low power consumption. For tactile applications and pressure measurements, they are applied in various fields from robotics to healthcare. In this context, flexible devices are very important for their high responsivity and ability to conform to the analyzed surface. This work reports on miniaturized flexible and compliant piezoelectric devices to increase the number of integrable sensors for detecting and discriminating localized pressures and contacts per unit area with minimal crosstalk. For this purpose, a series of aluminum nitride (AlN)-based piezoelectric sensors with different diameters (from 5 to 500 μm) was realized, and the generated electrical signal by sensor deformation was amplified by a differential voltage amplifier circuit. By the analysis of the shape of the piezoelectric signal as a function of the applied pressure, oscillations due to piezoelectric deformations, superimposed on the initial peak signal corresponding to the touch event, have been observed. The integral of the electrical signal was calculated for the most accurate representation to describe the sensor's response. The best responsivity was obtained in samples with diameters of 200 and 500 μm. Furthermore, it was also found that the minimum distance between the edges of closed sensors, observing crosstalk below −20 dB, was around 500 μm.**

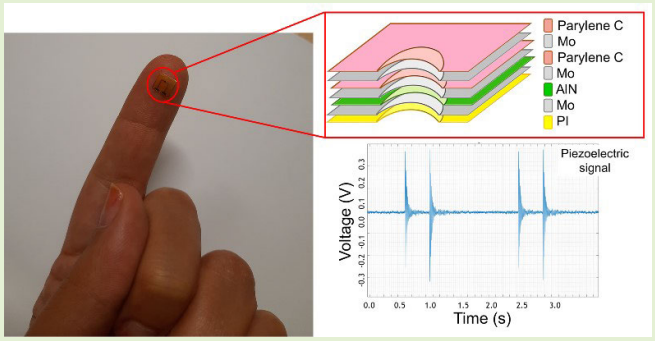

***Index Terms*— Microelectromechanical system (MEMS) devices, numerical integration of the electrical signal, piezoelectricity, pressure measurement, tactile sensors.**

I. Introduction

FLEXIBLE and wearable electronic devices can be used in several healthcare applications, including skin smart patches, motion detection, and remote healthcare [1], [2], [3]. In particular, in the latter case, they are useful for continuously monitoring human health parameters, such as heart beat rate, respiration rate, blood pressure, intracranial pressure, intraocular pressure, and limb movement in real time [4]. In recent years, the growing interest in soft robotics, industrial, and wearable medical applications has inspired the development of flexible microelectromechanical system (MEMS) sensors [5]. Pressure is one of the most important measured physical variables for monitoring biomechanical parameters useful for the diagnosis of pathologies related to cardiovascular muscular and motor problems [6]. Moreover, miniaturized pressure sensors could allow the realization of artificial skin for tactile prosthetics and robotics. Skin is a multilayered organ with the function to protect the human body; it can cushion the body from stress and strain, and perceive touch and heat [7], [8]. It, therefore, acts as a distributed sensor characterized by countless "active sensing areas," the nerve endings. To biomimic the high sensitivity of human skins, it is useful to increase the number of sensors that can be integrated per unit of the area [9], [10] on flexible substrates. This may be obtained by miniaturizing the pressure sensors, reducing the size of each sensor and allowing to collect, at the same time, the electrical signals produced in several points of a wearable distributed pressure-sensing substrate.

Pressure sensors are devices able to measure the pressures generated by the forces due to contact with external objects and their interactions with the surrounding environment. Therefore, they convert pressure into output electric signals

Manuscript received 15 February 2023; revised 29 March 2023; accepted 3 April 2023. Date of publication 13 April 2023; date of current version 15 May 2023. The associate editor coordinating the review of this article and approving it for publication was Dr. Jurgen Kosel. *(Corresponding author: F. Rizzi.)*

V. Carluccio, V. M. Mastronardi, and M. De Vittorio are with the Istituto Italiano di Tecnologia, Center for Biomolecular Nanotechnologies, 73010 Arnesano, Italy, and also with the Department of Innovation Engineering, University of Salento, 73100 Lecce, Italy (e-mail: Valeria.Carluccio@iit.it; VincenzoMariano.Mastronardi@unisalento.it; Massimo.DeVittorio@iit.it).

L. Fachechi, L. Natta, L. Algieri, G. de Marzo, and F. Rizzi are with the Istituto Italiano di Tecnologia, Center for Biomolecular Nanotechnologies, 73010 Arnesano, Italy (e-mail: Luca.Fachechi@iit.it; Lara.Natta@sicpa.com; Luciana.Algieri@iit.it; Gaia.DeMarzo@iit.it; Francesco.Rizzi@iit.it).

Digital Object Identifier 10.1109/JSEN.2023.3265871

according to the implemented transduction method. The most commonly used transduction methods in the pressure sensor field to convert mechanical displacements into electrical signals are piezoresistivity, capacitive transduction, and piezoelectricity. In piezoresistive sensors, the change in resistance is directly proportional to the strain caused by pressure on the sensor [11]. They do not require complex design, can be made at low cost, and are very resistant to impacts and vibrations, but, to work, they must be powered [8], [11], [12]. Capacitive pressure sensors measure changes in electrical capacitance caused by sensor deformation due to the applied pressure [11], [13]. They are mechanically simple, robust, and able to operate in a wide range of temperatures and pressures. However, they have reduced responsivity, are sensitive to vibrations [9], and exhibit a nonlinear response as the capacity is inversely proportional to the distance between the parallel electrodes [11]. One of the most suitable transduction principles to realize pressure sensors, which is able to directly convert applied mechanical energy into electrical signals, is based on piezoelectricity [9], [14]. The main advantages of piezoelectric devices are robustness, low power consumption, and downscaling [15]. In particular, piezoelectric materials require only a very small deformation to generate an output, so there are virtually no moving parts [16]. They are characterized by high responsivity, fast response time, and wide dynamic range. The sensor elements are self-powered; therefore, they are inherently low-power devices. From piezoelectric sensors, it is possible to generate an electrical signal by induced mechanical deformation and acquire it using an ad hoc readout circuit [17], [18], [19], [20], [21]. They are sensitive to changes in pressure, so the output voltage is usually treated as a relative pressure measurement, referenced to the initial state of the piezoelectric material. Therefore, the main characteristic of piezoelectric sensors is that they can only be used for dynamic pressure measurement.

To monitor biomechanical parameters through devices conformable to the body surface, conventional silicon (Si)-based MEMSs are inappropriate for their fragility and rigidity. Flexible and wearable piezoelectric sensors have several advantages: high adaptability to the body movements, ultralight weight, and extremely high responsivity [8], [12], [22], [23]. They are characterized by flexible substrates [22], [23], such as Kapton [24], polyimide (PI) [25], polyethylene naphthalate (PEN) [26], polyethylene terephthalate (PET) [27], and polydimethylsiloxane (PDMS) [28].

Several piezoelectric materials can be used to make flexible pressure sensors. On the one hand, perovskite structure piezoelectrics show good piezoelectric properties due to high-temperature curing treatments and poling processes [29]; however, it is very difficult to fabricate sensors with perovskite material directly on a flexible substrate. On the other hand, wurtzite structure piezoelectrics are biocompatible and nonferroelectric despite their moderate piezoelectric properties [29]. They are commonly used in MEMS devices and can be easily deposited on soft substrates as they do not need poling processes. Wurtzite piezoelectric materials include zinc oxide (ZnO) [30] and aluminum nitride (AlN) [25], [30]. The latter will be used in the realization of the sensors described in this work.

Furthermore, piezoelectric materials to be exploited for wearable and flexible pressure sensors are polymers such as polyvinylidene fluoride (PVDF) and its copolymer PVDF-trifluoroethylene (PVDF-TrFE). Piezoelectric polymers are semicrystalline organic materials with moderate piezoelectric constant, light, flexible, biocompatible, and can be easily deposited by electrospinning into thin films. However, they need mechanical stretching or high-voltage poling to develop their piezoelectricity [31]. Moreover, they are not compatible with standard CMOS technologies.

Piezoelectric sensors with relatively small sizes and low cost have been widely used in different application fields. Indeed, in recent years, the size of piezoelectric sensors has gradually decreased from a few centimeters to several hundred micrometers. For example, Chun et al. [27] in 2015 developed highly stretchable ZnO piezoelectric devices on a PET substrate with an active area of 1.5×1.5 cm^2. Jana et al. [28] made a piezoelectric device of PVDF on PDMS with an active area of 36×20 mm^2. Chen et al. [32] realized a piezoelectric sensor of PVDF-TrFE on a Kapton substrate with an active area of 2×0.4 cm^2. In 2016, several piezoelectric sensors were made with the following active areas 1×2.5 cm^2, 1.5×0.8 cm^2, and 5×13 mm^2 and, finally, one with an active area of about 22 mm^2 [33]. Todaro et al. [34] made piezoelectric flexible devices based on a thin film of AlN grown on a Kapton substrate having an active area of 2×2 mm^2. However, the difficulties encountered during microfabrication processes and the worsening of the performance at the low-scale piezoelectric sensors limit the possibility of obtaining pressure sensors with sizes that are too small [9].

In this article, we present a cluster of flexible tactile sensors characterized by a denser pitch with respect to the present literature, compatible with physiological constraints, and able to measure and map pressure for tactile applications [35]. To face this challenge, we first performed a systematic study in order to find the smallest sensor size to increase the sensor density. Then, we microfabricated clusters of miniaturized piezoelectric sensors in order to measure electromechanical properties and check reliability through crosstalk analysis.

For this purpose, we have realized a series of microfabricated flexible and wearable piezoelectric sensors varying their diameters from 5 to 500 μm in order to find the smallest sensor sizes able to preserve piezoelectric devices' functionality. The piezoelectric sensors exploit a sandwich structure based on an AlN thin film embedded between two layers of molybdenum (Mo) grown on a flexible substrate of PI. Moreover, we found the acceptable minimum allowable distance between sensors with minor cluster pitch.

In Section II-A, the characteristics of materials chosen to realize these devices have been presented. In Section II-A, the morphological, structural, crystallographic, and piezoelectric properties of AlN thin film have been related. In Section II-B, the fabrication processes used to realize these piezoelectric tactile sensors have be en presented. These piezoelectric

sensors, whose geometries were optimized by varying their diameters from 5 to 500 μm, are described in Section II-C. In Section III, the results of this work are presented. In particular, in Section III-A, piezoelectric sensors have been characterized electrically and electromechanically. In Section III-B, these sensors have been calibrated to detect electrical signals generated by sensor deformation. In Section III-C, the crosstalk analysis is presented by placing two or more sensors close to each other and detecting the minimum distance allowed between sensors such that the mechanical interference is negligible. After analyzing the shape of the piezoelectric signal generated, the conclusions drawn from this research are described in Section IV.

II. Materials and Methods

A. Choice of Materials

As a flexible growth substrate, a layer of PI 2555 has been chosen due to its low dielectric constant, excellent chemical stability, solvent resistance, high mechanical strength and stability, low stress, good thermal stability, and high glass transition temperature [36]. Moreover, PI can be directly deposited onto a Si wafer, by spin coating, resulting in a very flat surface and a good film thickness control, compatible with most common microfabrication processes.

Among piezoelectric materials, AlN has been selected and exploited to produce compact and efficient piezoelectric MEMS sensors due to its good mechanical properties and relatively low dielectric constant, despite its moderate piezoelectric coefficient [15]. In addition, AlN is an environmentally friendly and nontoxic ceramic material [37]; it exhibits high resistance to temperature and humidity, and can be directly deposited on soft substrates [38], making it useful to be implemented in flexible and wearable electronic devices.

Mo is one of the best metallic materials useful to realize thin film electrodes for MEMS devices [39]. It has many properties, including good adhesion to different substrates during the sputtering process, high melting point, relatively low thermal expansion coefficient, good thermal conductivity, corrosion, and oxidation resistance, despite a moderate value of electric conductivity [39], [40].

Among polymers adapted to mechanically protect and electrically insulate MEMS devices, parylene C was chosen because it is able to form an excellent protective barrier suitable for microfabricated electronic devices [41]. Parylene C has many attractive properties including biocompatibility, low gas permeability, anticorrosive behavior, and good adhesion on flexible substrates, such as PI and optimal conformability. Its coating process is very efficient, occurs at room temperature, allows complete control of the deposition parameters, and presents a significant etch rate in the oxygen plasma [39], [41].

B. Piezoelectric Material Characterization

To analyze the morphological, structural, and piezoelectric properties of an AlN film grown on a flexible substrate of PI 2555, a sample was made following the design shown in Fig. 1.

In particular, four layers of PI 2555 ($\approx$30 μm) have been deposited by spin coating on a Si wafer using a solution of

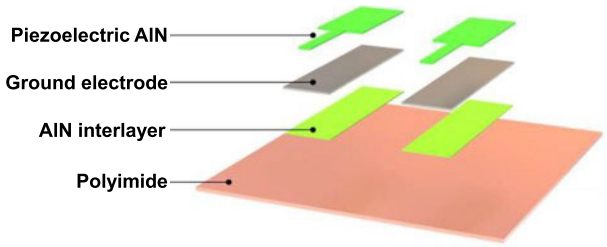

Fig. 1. Fabrication design of a piezoelectric stack of AlN-IL/Mo/AlN grown on PI 2555.

the VM651 adhesion promoter in the ratio of 1:10 in ethanol to improve the adhesion capacity of the polymer on the Si. The first three layers of PI have been cured on a hot plate at 130 °C for 5 min, while the fourth layer has been cured on the hot plate at 130 °C for 1 h. The PI curing has been completed with long curing at 200 °C for 2.5 h. This final PI curing temperature, even if it is not enough to obtain a full imidization, allowed us to obtain an adequately flexible substrate for tactile applications [42]. PI surface roughness has been increased by O_2 plasma using an Oxygen Plasma Asher to increase the adhesion of the bottom layer [25], [38]. Due to the amorphous or semiamorphous nature of the polymeric substrate, a thin film AlN-interlayer (AlN-IL) is deposited in order to improve adhesion properties and crystalline quality of the following piezoelectric active film (piezoelectric AlN in Fig. 1) [37]. To realize the intermediate bottom electrode, a layer of Mo has been chosen for its capability to promote the c-axis orientation of the AlN film. Therefore, a stack of AlN-IL (120 nm) and an Mo-bottom electrode (200 nm) have been deposited using a sputtering (Magnetron Sputtering, Kurt J. Lesker) instrument in the DC mode in a single run to minimize contaminations [43]. Later, a piezoelectric AlN thin film (900 nm) has been deposited on the whole sample area using the same instrument. The surface morphology of AlN thin film, grown on the PI layer, has been studied by atomic force microscopy (AFM) measurements (CSI Nano-Observer AFM), the structural properties have been investigated by a scanning electron microscope (SEM) (NanoLab 600i SEM/FIB, FEI), and the crystallographic properties and the quality of the AlN film have been analyzed by X-ray diffractometer (D8-Discover Bruker diffractometer, XRD). Piezoelectric properties and effective piezoelectric coefficient (d_{33}^{eff}) of AlN film have been evaluated by piezoresponse force microscopy (PFM) (CSI Nano-Observer AFM). According to the literature [25], by the AFM analysis, it has been obtained an average grain size equal to 42 nm and a roughness root mean square rms(sq)= 4.952 nm. To study the structural properties of this sample, a layer of Mo (200 nm) and a thin film of gold have been deposited on the AlN surface to improve the detection of backscattered electrons. By a cross section SEM analysis to monitor the grain structure of the AlN film, a columnar grain structure has been observed [44]. By X-ray diffraction, the spectrum in $\vartheta/2\vartheta$ configuration has been observed with a diffraction peak centered at 36°, corresponding to (002) crystal orientation of the AlN wurtzite structure and a peak centered at 40.55° due to the Mo bottom layer with orientation along

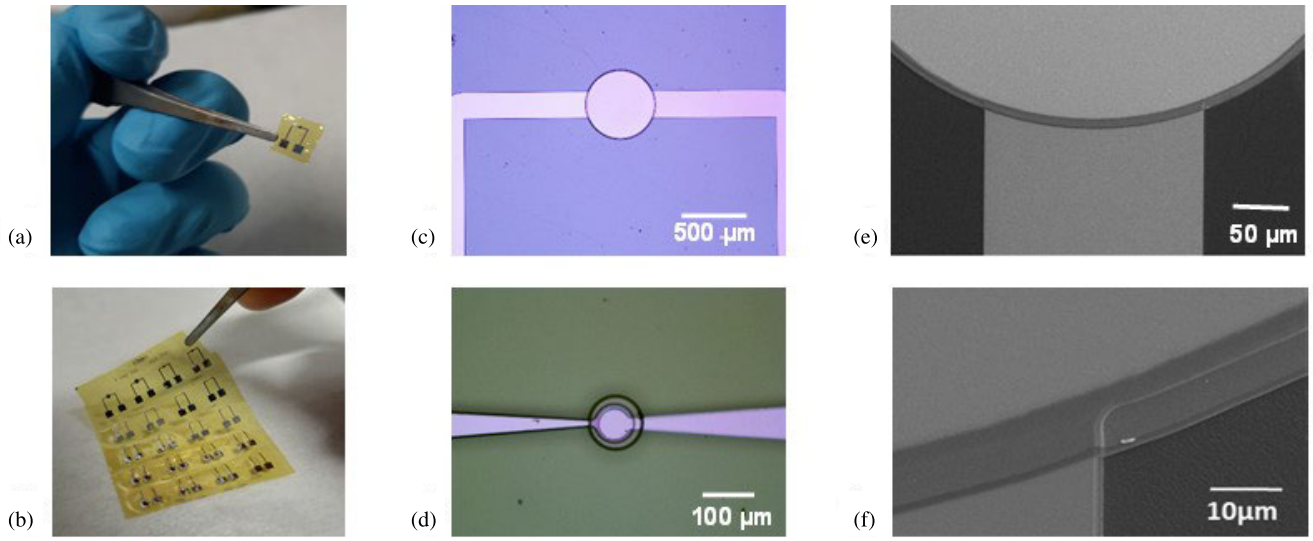

Fig. 2. (a) Single flexible device detached. (b) Series of different sensors varying their diameter. (c) Optical microscope image of 500 μm. (d) 50-μm-diameter sample. (e) SEM images of a piezoelectric tactile sensor viewed without a tilt angle. (f) Viewed with a tilt angle of 52°.

the (110) plane [45]. The piezoelectric properties and the effective piezoelectric coefficient (d_{33}^{eff}) of AlN grown on PI have been evaluated using piezoresponse force microscopy (PFM). To make the AlN sample suitable for PFM, a layer of Kapton tape has been used, during dielectric sputtering growth and then removed, to expose part of the Mo bottom electrode. For this structure, it has been found an effective piezoelectric coefficient $d_{33}^{\text{eff}} \approx 4.5$ pm/V, in accordance with the literature [25].

C. Fabrication and Characterization of Piezoelectric Tactile Sensors

Starting from these material characterizations, a flexible piezoelectric sample characterized by an Mo/AlN/Mo thin film heterostructure was made on a PI substrate using reactive sputtering UV-lithography and dry etching.

To make the sensors detachable from the Si substrate, a sacrificial layer of polymer polymethylmethacrylate (PMMA) has been spun, and a layer of VM651 adhesion promoter has been spun to promote PI adhesion to the substrate [42]. A layer around 30-μm-thick PI has been deposited by spin coating on an Si wafer, and its surface roughness has been increased by O_2 plasma, as described in the previous paragraph.

The sputtered stack is characterized by an AlN-IL (120 nm) and bottom Mo electrode (200 nm) deposited in a single run, a layer of piezoelectric AlN (1.5 μm), and a top Mo electrode (200 nm). The fabrication processes used to realize this heterostructure are reported in the literature [15], [24], [25], [37], [46]. In particular, the deposition parameters for the two AlN layers (interlayer and piezoelectric layer) are a gas mixture of N_2 (20 sccm)/Ar (20 sccm) at a pressure of 0.002 mbar and a power of 1250 W, while the two Mo layers (top and bottom electrodes) are deposited in an Ar atmosphere (65 sccm) at a pressure of 0.005 mbar and a power of 200 W.

Later, a metal layer embedded between two layers of parylene C has been added to the stack top surface [37]. This particular layer works as an electromagnetic shield to reduce the noise and enhance the signal-to-noise ratio. The second layer of parylene C (thickness: 2 μm) has been added to mechanically protect and electrically insulate the sensors, completing the passivation microfabrication step. The first layer of parylene has a thickness of about 1 μm, and the second one is about 2 μm. The shield electrode in between, patterned using the liftoff technique, is made by a 20-nm-thick titanium (Ti) layer (deposition parameters: 30 sccm of Ar with 0.0025-mbar pressure and 400-W power) and a 400-nm-thick Mo layer (deposition parameters: 65 sccm of Ar with 0.005-mbar pressure and 200-W power). The thin film of Ti is needed to improve the adhesion ability of Mo on the first layer of parylene.

The release/detachment of the devices from the rigid support of Si has been performed by cleaving the edges with a razor blade and dipping the sample in acetone. After a few minutes, the PI layer has been detached by the Si wafer, obtaining a flexible sample that has been used in this work [see Fig. 2(a)].

In this way, a series of different piezoelectric sensors have been realized varying their size from 5 to 500 μm in diameter, as shown in Fig. 2(b). In Fig. 2(c) and (d), the optical microscope images of 500- and 50-μm diameter samples are shown, respectively. In Fig. 2(e) and (f), SEM images of a piezoelectric tactile sensor without a tilt angle and with a tilt angle of 52° are shown, respectively.

The electrical properties of the produced sensors have been evaluated by measuring the capacitance and impedance of each sensor before and after the release process. These physical quantities have been measured using an *LCR* meter (Agilent E4980A) at a frequency of 1 kHz by applying a source voltage of 3 V [43]. The electromechanical properties of our sensors have been obtained using a laser Doppler vibrometer (LDV, Polytec Vibrometer MSA-500) by exciting them electrically and detecting their deformation as a function of frequency. Finally, our piezoelectric sensor performance has been calibrated using a pull/shear tester (XYZTEC Condor EZ) [15],

which applies a repeatable normal deformation in time onto each piezoelectric sensor. The electrical signal produced by the sensor deformation is detected on an oscilloscope via a differential voltage amplifier circuit.

III. Results and Discussion

A. Electrical and Electromechanical Characterization of Piezoelectric Tactile Sensors

The AlN-based piezoelectric sensors' configuration consists of a parallel plate capacitor, which is possible to measure the capacitance and impedance values using an *LCR* meter. It is known that

$$C = \frac{\varepsilon_0 \varepsilon_r S}{d} \tag{1}$$

and

$$Z_c = \frac{1}{2\pi f C} \tag{2}$$

where C (in F) is the capacitance of the sensor with active area S (in m^2), ε_0 is the permittivity of free space, ε_r is the AlN permittivity, and d is the AlN thin film thickness. Z_c (in Ω) is the sensor impedance, and f is the frequency at which these electrical measurements were carried out. Capacitance and impedance values have been measured for each device with a diameter ranging from 5 to 500 μm, before and after the release process from the substrate.

The electrical parameters of our samples have been evaluated and shown in Fig. 3(a) and (b). Samples with an active area diameter equal to 5 and 10 μm showed capacitance and impedance values very far from the theoretically expected values. In particular, for these samples, C and Z_c behaviors showed a plateau. Indeed, for reduced diameters of the realized circle, the size of the effective active area remained almost constant due to the nonnegligible contributions of the lateral surface electrode. Moreover, a parasitic resistance (losses) in parallel with the capacitance lowered the total impedance value, mainly when capacitance was very low, because, in this case, the reactive impedance was very high. In contrast, the sensors with diameters greater than 10 μm (from 20 up to 500 μm) had capacitance and impedance values compatible with those theoretically expected. In particular, the expected impedance values ranged from 2.4 GΩ for the smallest samples to about 10 MΩ for the largest ones. Smaller impedance values are more suitable for the design of the signal conditioning circuits.

Furthermore, the electromechanical properties of the proposed sensors have been evaluated using an LDV, and frequency spectra with a large band [47] below 40 kHz have been observed. In particular, Fig. 3(c) shows the frequency spectrum of the sample with a diameter of 100 μm obtained by electrically exciting the sample. Two resonance peaks are observed for it: one around 10 kHz (10 156 Hz) and the other around 19 kHz (18 719 Hz). Exciting the sample at these frequencies, it has been observed the vibration modes shown in Fig. 3(d) and (e).

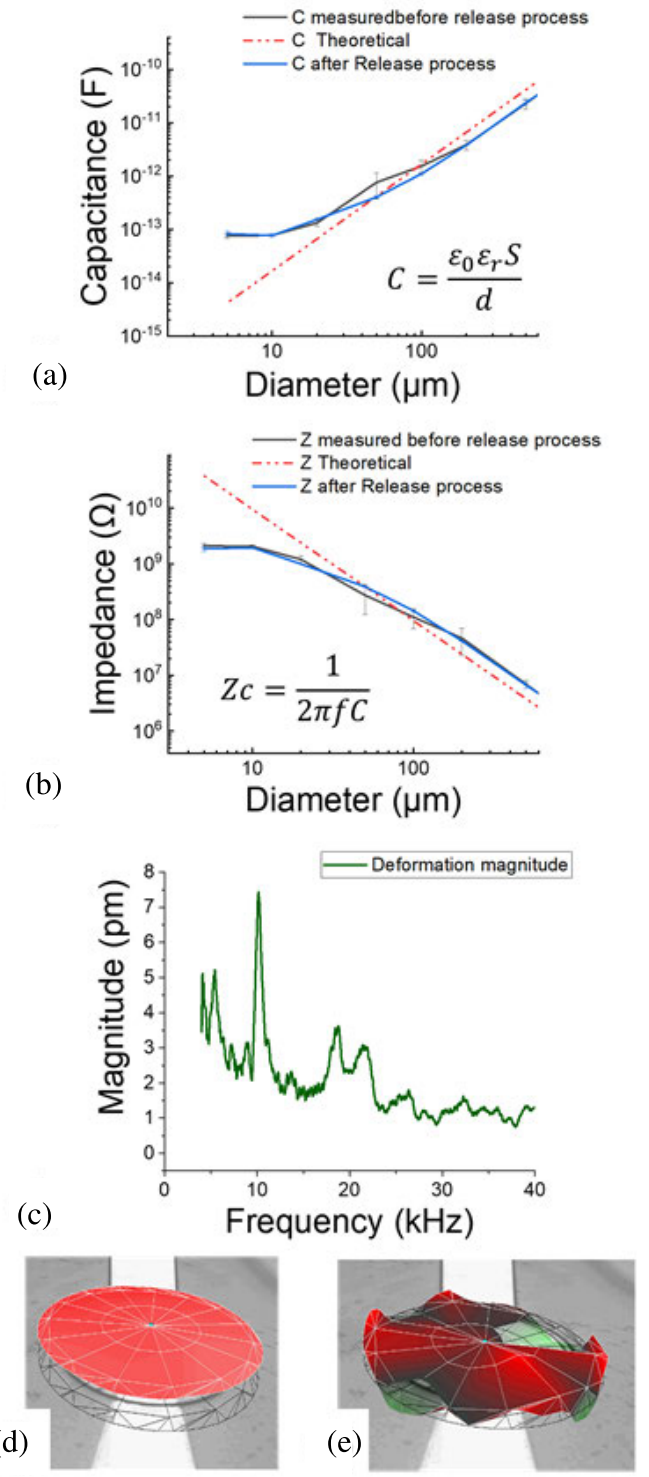

Fig. 3. Electrical characterization before and after the release process: (a) capacitance measurements and (b) impedance measurements. (c)–(e) Electromechanical characterization of the sensor with a diameter of 100 μm.

B. Calibration of Piezoelectric Tactile Sensors

To study the contact interactions between the developed sensors and external objects, an impact test was performed using a pull/shear tester machine (XYZTEC Condor EZ). This instrument includes a motion-controlled single head equipped

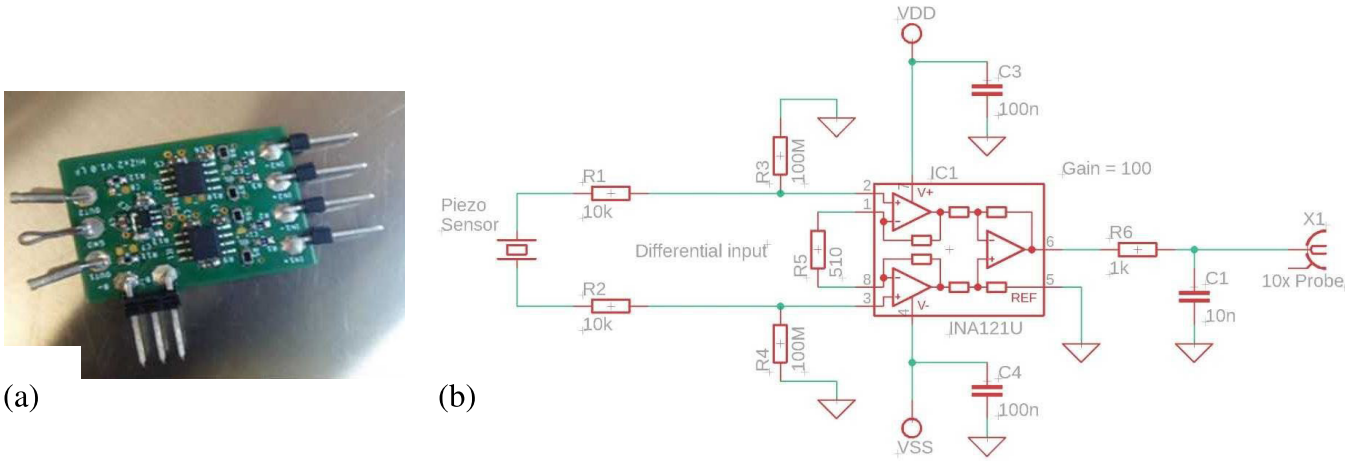

Fig. 4. (a) Image of a differential voltage amplifier circuit and (b) related circuit diagram used in this work.

with a force sensor for push and pull tests. A small metal rod, almost 500 μm in diameter, was used to apply a repeatable normal force in time and produces a normal deformation of the tested flexible piezoelectric sensors. During the impact test, the probe was optically aligned with the center of each sensor. This calibration was in a quasi-static regime [48] with a test velocity of 1.5 mm/s. The head was placed at a defined distance from the device. First, the head was moved to go in touch with the device under test, defining the initial touch position. Then, the moving distance of the head was increased by a step of 1 μm. Before starting the test, the instrument was calibrated as the measurement can be influenced by the deformation of the thin metal tool. The deformation of the tool is included in the calculation of the force versus displacement calibration curve considering the compliance of the tool by the following equation:

$$\delta_t = P^* C_t \tag{3}$$

where δ_t is the deformation of the tool, P is the load, and C_t is the tool compliance. Therefore, the following equation:

$$\delta = \delta_m - \delta_t \tag{4}$$

becomes

$$\delta = \delta_m - P * C_t \tag{5}$$

where δ is the wanted deformation, δ_m is the measured deformation, and δ_t is the deformation of the tool [49]. These equations were used to take into account tool compliance. Each sensor was connected to an oscilloscope via a differential voltage amplifier circuit, and the electrical signal generated by the deformation of each flexible piezoelectric sensor under the action of the pull/shear probe was detected.

The two-channel differential voltage amplifier, as shown in Fig. 4(a) and (b), is built around an instrument amplifier, which has low input noise (20 nV/$\sqrt{}$Hz) and a wide supply range ($\pm$18 V). The amplification factor can be set by only one resistor and can span from $\mathbf{x}1$ to $\mathbf{x}10^4$. The high differential input impedance and differential low input capacitance (10^{12} Ω|| 1 pF) and low bias current (4 pA) allow making a very high input impedance amplifier, here $\sim$100 MΩ, which can amplify signals from high-impedance sources, such as piezoelectric sensors. Moreover, differential input allows make measurements not referred to the ground and to measure concurrently two independent source voltages. Fig. 5 shows the electrical signal read on the oscilloscope for a sensor with a diameter of 500 μm using the differential voltage amplifier described above. It represents the typical piezoelectric behavior of all sensors [41], [50], [51], [52]. The piezoelectric signal is characterized by two parts with opposite signs, related to the two processes of touch and release, in a single occurring cycle [53], respectively. In particular, during the forward touch step, the sensor is deformed, and an increase in the detected electric signal is observed due to the electrical charge produced by the piezoelectric effect (positive electrical potential in Fig. 5). In the release step, the material is deformed in the opposite direction; therefore, charge opposite to the previous one is generated, and an electric potential opposite to that of the touch step is detected (negative electrical potential in Fig. 5). In the intermediate phase, since the metallic post is no longer moving, there are no variations in the deformation of the material, and no electric potential is detected from the piezoelectric effect [41], [54]. Using the pull/shear tester described above, it is possible to obtain the calibration curves for each sample with a diameter from 20 to 500 μm, detecting the peak-to-peak electrical voltage as a function of applied force. Then, dividing the force values by the active area of each sensor, the normalized calibration curves, peak-to-peak voltage versus pressure, were calculated. By this preliminary test, an apparent linear proportionality between the electrical signal generated and the diameter of each sample at a fixed pressure equal to 12.6 kPa has been observed [see Fig. 5(c)] [55]. From the calibration curves of voltage versus pressure, responsivity and dynamic range values have been calculated. Responsivity is the slope of voltage versus pressure calibration curves, while the dynamic range is defined as the ratio between the maximum and minimum values of the detected pressure.

Responsivity values range from 5×10^{-6} V/kPa for the smaller sensor (20-μm-diameter sensor) to 5×10^{-1} V/kPa for the larger one (500-μm-diameter sensor). This dependence

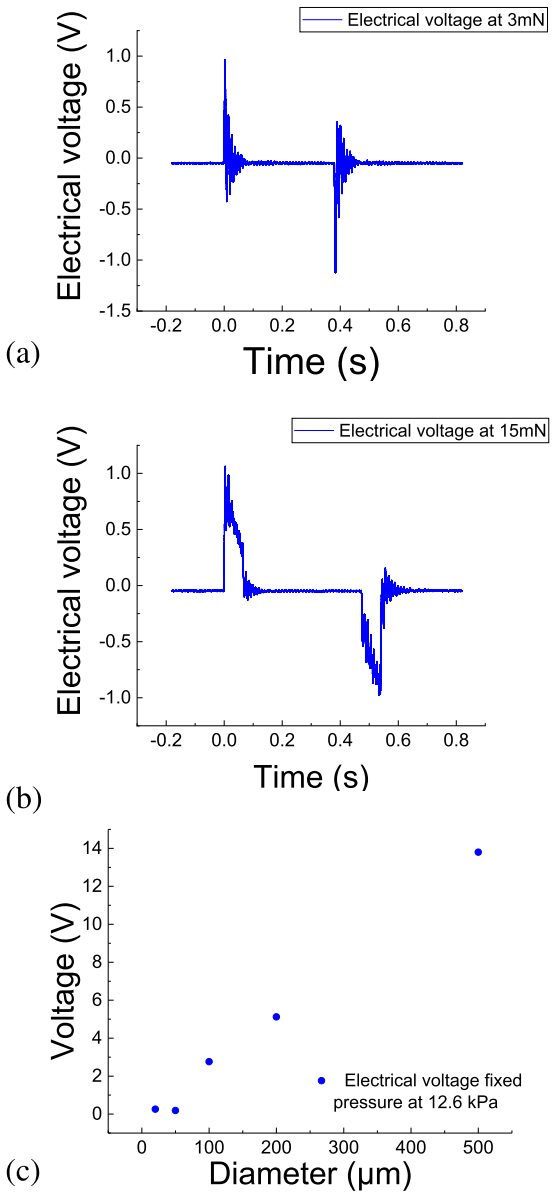

Fig. 5. (a) Electrical signal shape at low force (≈3 mN) for a 500-μm-diameter sensor, (b) at high force (≈15 mN) for the same sensor, and (c) plot of voltage versus sensors diameter with the pressure fixed at 12.6 kPa.

on the sensor diameter could be explained by the interaction between the piezoelectric membrane and the impact tester tool, which has a constant diameter of about 500 μm. When in contact with smaller membrane diameters, the border effect could result in lower signals. In the calculation of the dynamic range, it is assumed that the response (V) tends to zero when the excitation (P) tends to zero. To detect these calibration curves, each sensor has been connected to a differential voltage amplifier circuit with an input impedance of about 100 MΩ. To enhance the dynamic range of our sensor's calibration curves, an alternative approach was based on the analysis of the generated electrical signal shape as a function of the applied force/pressure. From Fig. 5(a) and (b), the piezoelectric signal is characterized by an oscillation overlapped on the peak signal due to the deformations of the piezoelectric. During the measurement, the pull/shear tool moves downward at a constant speed equal to 1.5 mm/s applying an increasing deformation to the sensor membrane with time. At higher deformations, stronger forces correspond. Since the speed of the tool is constant, the interaction time between the tool and the sample increases with the desired target force. The force is not linear with tool displacement due to the nonlinear compression of the polymeric substrate. This explains why the duration of the peak in Fig. 5(a) (≈75 ms at 3 mN) is shorter than that of the peak in Fig. 5(b) (≈160 ms at 15 mN). Moreover, the oscillations overlapped to and following the main signals are induced by membrane mechanical oscillations. Through this analysis, it was considered that the best way to describe our sensors' response was not to detect the peak-to-peak voltage but to calculate the integral of the whole signal. Then, through that approach in which the signal was numerically integrated with a signal postprocessing phase, the new calibration curves have been calculated for each sensor, and a new dynamic range was calculated reaching values up to an order of magnitude higher than previously obtained. Indeed, the value of the dynamic range increased from about 10 to about 100. Normalizing each curve to the sensor area, we found the calibrations shown in Fig. 6(a). For each calibration curve, the parameters of responsivity, dynamic range, sensitivity, and signal-to-noise ratio have been calculated. We have observed that responsivity increases nonlinearly as the sensor size increases [see Fig. 6(b)]. Moreover, we found that the best samples in terms of responsivity are those with active area diameters of 200 and 500 μm. By the calibration curves reported in Fig. 6, the responsivity and the pressure interval for the samples with an active area diameter equal to 200 and 500 μm assume the following values 0.001 Vs/kPa, 314 kPa and 0.015 Vs/kPa and 36.5 kPa, respectively.

To the best of our knowledge, the sensors presented in this article have a lower active area than other piezoelectric sensors in the literature [50], [56], [57], [58], [59]. A comparison of flexible piezoelectric sensors in terms of active area and piezoelectric coefficient value is reported in Table I. It results that the sensor object of this article is the smallest among others. This is useful in tactile/biomedical applications [60], and they are suitable for integration in clusters of sensors allowing finer detection.

C. Crosstalk Analysis

The minimum distance between sensors such that the mechanical crosstalk is equal to −20 dB was investigated. For this purpose, AlN sensors have been placed at different distances from each other on the same flexible substrate [see Fig. 7(a)]. To perform the crosstalk analysis, the ratio between the signal detected from a sensor, not in contact with the pull/shear probe, and that of the excited one was measured. The crosstalk values for each distance between the edges of each couple of sensors (0.2, 0.5, and 1 and 1.12 mm) were measured. The graph reported in Fig. 7(b) shows how much the crosstalk decreases as the relative distance between the sensors increases when the force of 10 mN is applied to one

TABLE I
COMPARISON OF FLEXIBLE PIEZOELECTRIC SENSORS IN TERMS OF ACTIVE AREA AND PIEZOELECTRIC COEFFICIENT VALUE

References	Active material	Piezoelectric coefficient (pm/V)	Active Area (mm^2)	Application field
Lee [56]	ZnO on Al-foil	5.5 – 12.4	65	Motion sensing
Tseng [57]	PZT on flexible stainless steel substrate	90 – 223 (after poling)	3	Biomedical monitoring
Yu [58]	PVDF on PDMS	30 (after poling)	2.25	Tactile sensing
Dahiya [59]	PVDF-TrFE on Si	30 (after poling)	1	Tactile sensing
Kumaresan [50]	AlN on Ultra-thin Si	5	0.5	Tactile sensing
This work	AlN on PI	4.5	0.196 0.03	Tactile sensing

PZT = Lead Zirconate Titanate

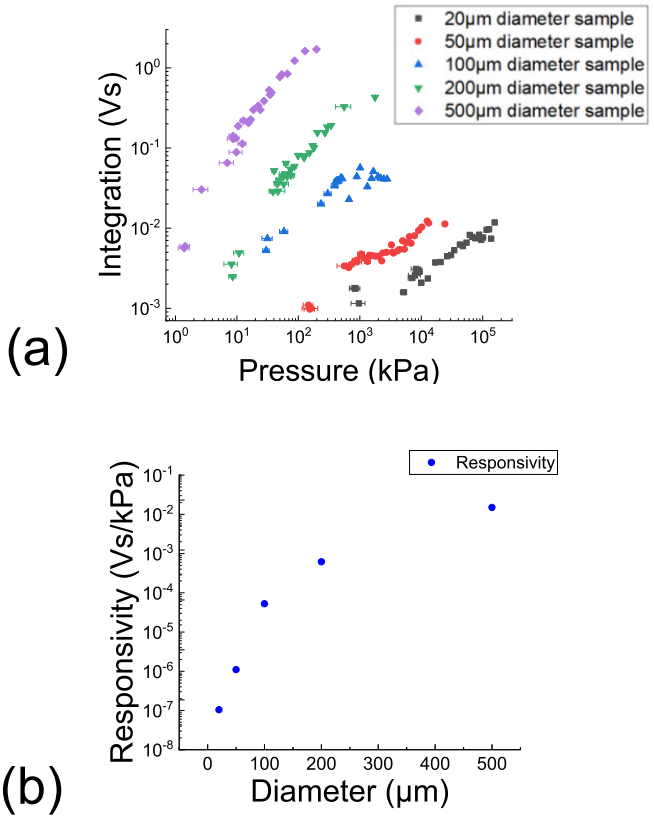

Fig. 6. (a) Integral of electrical signal (Vs) versus pressure (kPa) and (b) responsivity as a function of sensors diameter for the calibration curves.

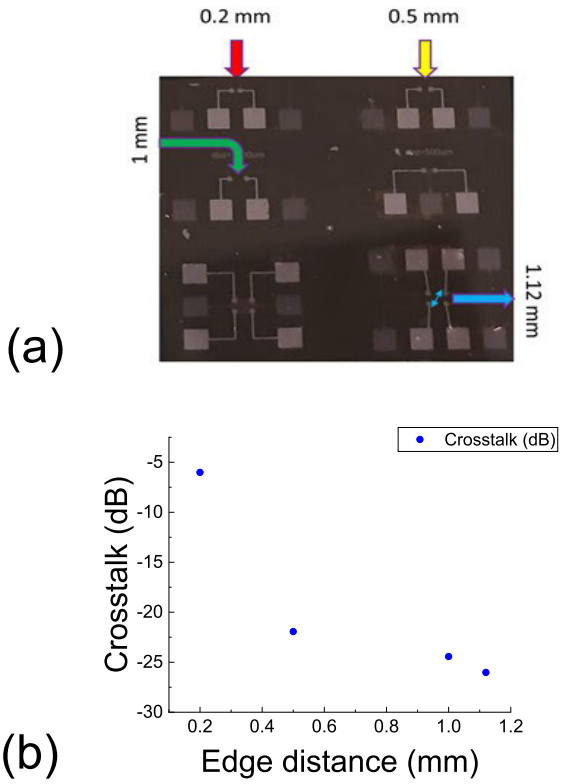

Fig. 7. (a) Crosstalk samples with relative distance between sensors edges and (b) crosstalk values versus distance between sensors.

sensor of the cluster. If the distance between the sensors is at least 0.5 mm, the signal produced by the excited sensor is an order of magnitude greater than the unexcited one with crosstalk equal to −20 dB.

IV. CONCLUSION

In this work, flexible and wearable microfabricated piezoelectric pressure sensors with high sensitivity for tactile applications have been realized. These microsystems could be able to monitor fine and small grasping movements using an ad hoc realized conditioning system. After characterizing

the morphological and structural properties of the chosen piezoelectric material (AlN), a series of flexible piezoelectric sensors with a diameter ranging between 5 and 500 μm has been realized. The smallest sensor size, about 20 μm, able to preserve piezoelectric devices functionality has been identified. Through the electrical characterization of these sensors, it has been observed that those with a diameter ranging from 20 up to 500 μm show an electrical behavior compatible with that expected. A linear relationship between the electrical signal generated and the diameter of each sample at a fixed pressure was observed. Analyzing the shape of the output electric signal in function of the applied pressure, calibration curves have been obtained by exploiting the numerical integration of the sensor output. For the sensors with an active area diameter equal to 200 and 500 μm, the values of responsivity and dynamic range have been calculated as 0.001 Vs/kPa, 314 kPa and 0.015 Vs/kPa and 36.5 kPa, respectively. These sensors have an active area of less than 0.2 mm^2, improving the previous state of the art in terms of device miniaturization. From crosstalk analysis, it was found that the minimum distance between sensors with $-$20-dB crosstalk is around 0.5 mm, suggesting that this is a safe distance for tactile applications. Moreover, the signal processing from piezoelectric membranes introduced in this work based on the numerical integration during the calibration phase and allowing for an increase in the dynamic range of miniaturized pressure sensors has not yet been exploited previously. The improvements in responsivity and dynamic range suggest exploiting this integration method to directly calibrate piezoelectric sensors and monitor the electrical signal during the fine and small movements involved in grasping and manipulation activities.

REFERENCES

[1] K. Takei, W. Honda, S. Harada, T. Arie, and S. Akita, "Toward flexible and wearable human-interactive health-monitoring devices," *Adv. Healthcare Mater.*, vol. 4, no. 4, pp. 487–500, Mar. 2015.

[2] G. Ge, W. Huang, J. Shao, and X. Dong, "Recent progress of flexible and wearable strain sensors for human-motion monitoring," *J. Semicond.*, vol. 39, no. 1, Jan. 2018, Art. no. 011012.

[3] Y. Gu et al., "Mini review on flexible and wearable electronics for monitoring human health information," *Nanosc. Res. Lett.*, vol. 14, no. 1, Aug. 2019, Art. no. 263.

[4] J. Chen et al., "Bioinspired design of highly sensitive flexible tactile sensors for wearable healthcare monitoring," *Mater. Today Chem.*, vol. 23, Mar. 2022, Art. no. 100718.

[5] S. Beeby, G. Ensel, and N. M. White, *MEMS Mechanical Sensors*. Norwood, MA, USA: Artech House, 2004.

[6] P. Saccomandi et al., "Microfabricated tactile sensors for biomedical applications: A review," *Biosensors*, vol. 4, no. 4, pp. 422–448, Dec. 2014.

[7] W. Lin, B. Wang, G. Peng, Y. Shan, H. Hu, and Z. Yang, "Skin-inspired piezoelectric tactile sensor array with crosstalk-free row+column electrodes for spatiotemporally distinguishing diverse stimuli," *Adv. Sci.*, vol. 8, no. 3, Feb. 2021, Art. no. 2002817.

[8] X. Wang, L. Dong, H. Zhang, R. Yu, C. Pan, and Z. L. Wang, "Recent progress in electronic skin," *Adv. Sci.*, vol. 2, no. 10, Oct. 2015, Art. no. 1500169.

[9] P. Song et al., "Recent progress of miniature MEMS pressure sensors," *Micromachines*, vol. 11, no. 1, p. 56, Jan. 2020.

[10] M. K. Mishra, V. Dubey, P. M. Mishra, and I. Khan, "MEMS technology: A review," *J. Eng. Res. Rep.*, vol. 4, no. 1, pp. 1–24, Feb. 2019.

[11] F. Xu et al., "Recent developments for flexible pressure sensors: A review," *Micromachines*, vol. 9, no. 11, p. 580, Nov. 2018.

[12] Y. Gao et al., "Wearable microfluidic diaphragm pressure sensor for health and tactile touch monitoring," *Adv. Mater.*, vol. 29, no. 39, Oct. 2017, Art. no. 1701985.

[13] M. Su, P. Li, X. Liu, D. Wei, and J. Yang, "Textile-based flexible capacitive pressure sensors: A review," *Nanomaterials*, vol. 12, no. 9, p. 1495, Apr. 2022.

[14] A. D. Santos, E. Fortunato, R. Martins, H. Águas, and R. Igreja, "Transduction mechanisms, micro-structuring techniques, and applications of electronic skin pressure sensors: A review of recent advances," *Sensors*, vol. 20, no. 16, p. 4407, Aug. 2020.

[15] V. M. Mastronardi et al., "Low stiffness tactile transducers based on AlN thin film and polyimide," *Appl. Phys. Lett.*, vol. 106, no. 16, Apr. 2015, Art. no. 162901.

[16] N.-I. Kim et al., "Piezoelectric pressure sensor based on flexible gallium nitride thin film for harsh-environment and high-temperature applications," *Sens. Actuators A, Phys.*, vol. 305, Apr. 2020, Art. no. 111940.

[17] W. Choi, J. Lee, Y. K. Yoo, S. Kang, J. Kim, and J. H. Lee, "Enhanced sensitivity of piezoelectric pressure sensor with microstructured polydimethylsiloxane layer," *Appl. Phys. Lett.*, vol. 104, no. 12, Mar. 2014, Art. no. 123701.

[18] Y. Yuan et al., "Highly sensitive and wearable bionic piezoelectric sensor for human respiratory monitoring," *Sens. Actuators A, Phys.*, vol. 345, Oct. 2022, Art. no. 113818.

[19] Y. Du et al., "Hybrid printing of wearable piezoelectric sensors," *Nano Energy*, vol. 90, Dec. 2021, Art. no. 106522.

[20] I. Cesini et al., "Seedless hydrothermal growth of ZnO nanorods as a promising route for flexible tactile sensors," *Nanomaterials*, vol. 10, no. 5, p. 977, May 2020.

[21] L. Pinna, A. Ibrahim, and M. Valle, "Interface electronics for tactile sensors based on piezoelectric polymers," *IEEE Sensors J.*, vol. 17, no. 18, pp. 5937–5947, Sep. 2017.

[22] M. Ha, S. Lim, and H. Ko, "Wearable and flexible sensors for user-interactive health-monitoring devices," *J. Mater. Chem. B*, vol. 6, no. 24, pp. 4043–4064, 2018.

[23] Y. Wu, Y. Ma, H. Zheng, and S. Ramakrishna, "Piezoelectric materials for flexible and wearable electronics: A review," *Mater. Des.*, vol. 211, Dec. 2021, Art. no. 110164.

[24] L. Natta et al., "Conformable AlN piezoelectric sensors as a non-invasive approach for swallowing disorder assessment," *ACS Sensors*, vol. 6, no. 5, pp. 1761–1769, May 2021.

[25] L. Algieri et al., "Flexible piezoelectric energy-harvesting exploiting biocompatible AlN thin films grown onto spin-coated polyimide layers," *ACS Appl. Energy Mater.*, vol. 1, no. 10, pp. 5203–5210, Oct. 2018.

[26] L. Piro et al., "Flexible SAW microfluidic devices as wearable pH sensors based on ZnO nanoparticles," *Nanomaterials*, vol. 11, no. 6, p. 1479, Jun. 2021.

[27] J. Chun et al., "Highly anisotropic power generation in piezoelectric hemispheres composed stretchable composite film for self-powered motion sensor," *Nano Energy*, vol. 11, pp. 1–10, Jan. 2015.

[28] S. Jana, S. Garain, S. Sen, and D. Mandal, "The influence of hydrogen bonding on the dielectric constant and the piezoelectric energy harvesting performance of hydrated metal salt mediated PVDF films," *Phys. Chem. Chem. Phys.*, vol. 17, no. 26, pp. 17429–17436, 2015.

[29] C. B. Eom and S. Trolier-Mckinstry, "Thin-film piezoelectric MEMS," *MRS Bull.*, vol. 37, no. 11, pp. 1007–1017, Nov. 2012.

[30] A. Fraleoni-Morgera, I. Cesini, P. Kumar, and C. M. Oddo, "Hydrothermally grown ZnO nanorods as promising materials for low cost electronic skin," *ChemNanoMat*, vol. 6, no. 1, pp. 15–31, Jan. 2020.

[31] D. Tadaki et al., "Piezoelectric PVDF-based sensors with high pressure sensitivity induced by chemical modification of electrode surfaces," *Sens. Actuators A, Phys.*, vol. 316, Dec. 2020, Art. no. 112424.

[32] D. Chen, T. Sharma, and J. X. J. Zhang, "Mesoporous surface control of PVDF thin films for enhanced piezoelectric energy generation," *Sens. Actuators A, Phys.*, vol. 216, pp. 196–201, Sep. 2014.

[33] C. Dagdeviren et al., "Recent progress in flexible and stretchable piezoelectric devices for mechanical energy harvesting, sensing and actuation," *Extreme Mech. Lett.*, vol. 9, pp. 269–281, Dec. 2016.

[34] M. T. Todaro et al., "Biocompatible, flexible, and compliant energy harvesters based on piezoelectric thin films," *IEEE Trans. Nanotechnol.*, vol. 17, no. 2, pp. 220–230, Mar. 2018.

[35] J. J. Zárate, G. Tosolini, S. Petroni, M. De Vittorio, and H. Shea, "Optimization of the force and power consumption of a microfabricated magnetic actuator," *Sens. Actuators A, Phys.*, vol. 234, pp. 57–64, Oct. 2015.

[36] A. Lin, "Evaluation of polyimides as dielectric materials for multichip packages with multilevel interconnection structure," *IEEE Trans. Compon., Hybrids, Manuf. Technol.*, vol. 13, no. 1, pp. 207–213, Mar. 1990.

[37] F. Guido, A. Qualtieri, L. Algieri, E. D. Lemma, M. De Vittorio, and M. T. Todaro, "AlN-based flexible piezoelectric skin for energy harvesting from human motion," *Microelectron. Eng.*, vol. 159, pp. 174–178, Jun. 2016.

[38] N. Jackson, L. Keeney, and A. Mathewson, "Flexible-CMOS and biocompatible piezoelectric AlN material for MEMS applications," *Smart Mater. Struct.*, vol. 22, no. 11, Oct. 2013, Art. no. 115033.

[39] K. R. Williams, K. Gupta, and M. Wasilik, "Etch rates for micromachining processing—Part II," *J. Microelectromech. Syst.*, vol. 12, no. 6, pp. 761–778, Dec. 2003.

[40] V. A. Volkovich, A. B. Ivanov, R. V. Kamalov, D. S. Maltsev, B. D. Vasin, and T. R. Griffiths, "Electrode and redox potentials of molybdenum and stability of molybdenum chloro-species in alkali chloride melts," *J. Electrochem. Soc.*, vol. 164, no. 8, pp. H5336–H5344, Jul. 2017.

[41] M. Mariello, L. Fachechi, F. Guido, and M. De Vittorio, "Multifunctional sub-100 μm thickness flexible piezo/triboelectric hybrid water energy harvester based on biocompatible AlN and soft parylene C-PDMS-ecoflex^{TM}," *Nano Energy*, vol. 83, May 2021, Art. no. 105811.

[42] L. Natta et al., "Soft and flexible piezoelectric smart patch for vascular graft monitoring based on aluminum nitride thin film," *Sci. Rep.*, vol. 9, no. 1, pp. 1–10, Jun. 2019.

[43] V. M. Mastronardi, F. Guido, M. Amato, M. De Vittorio, and S. Petroni, "Piezoelectric ultrasonic transducer based on flexible AlN," *Microelectron. Eng.*, vol. 121, pp. 59–63, Jun. 2014.

[44] C. Han et al., "High potential columnar nanocrystalline AlN films deposited by RF reactive magnetron sputtering," *Nano-Micro Lett.*, vol. 4, no. 1, pp. 40–44, Mar. 2012.

[45] S. S. Chauhan, M. M. Joglekar, and S. K. Manhas, "Influence of process parameters and formation of highly c-Axis oriented AlN thin films on mo by reactive sputtering," *J. Electron. Mater.*, vol. 47, no. 12, pp. 7520–7530, Sep. 2018.

[46] L. Natta et al., "Aluminium nitride based bio-MEMS for vascular graft monitoring," in *Proc. EMPC*, Pisa, Italy, Sep. 2019, pp. 1–6.

[47] E. Scarpa et al., "Wearable piezoelectric mass sensor based on pH sensitive hydrogels for sweat pH monitoring," *Sci. Rep.*, vol. 10, no. 1, pp. 1–10, Jul. 2020.

[48] A. Gaiardo, D. Novel, E. Scattolo, A. Bucciarelli, P. Bellutti, and G. Pepponi, "Dataset of the optimization of a low power chemoresistive gas sensor: Predictive thermal modelling and mechanical failure analysis," *Data*, vol. 6, no. 3, p. 30, Mar. 2021.

[49] C. Gabry, "Investigation of the structural resistance of silicon membranes for microfluidic applications in high energy physics," M.S. thesis, EPFL, Lausanne, Switzerland, 2014.

[50] Y. Kumaresan et al., "AlN ultra-thin chips based flexible piezoelectric tactile sensors," in *Proc. FLEPS*, Manchester, U.K., 2021, pp. 1–4.

[51] Y. Luo et al., "A flexible tactile sensor for three-dimensional force detection based on piezoelectric sensing," in *Proc. IEEE 16th Int. Conf. Nano/Micro Eng. Mol. Syst. (NEMS)*, Apr. 2021, pp. 1908–1911.

[52] J. Jiang et al., "Flexible piezoelectric pressure tactile sensor based on electrospun $BaTiO_3$/poly(vinylidene fluoride) nanocomposite membrane," *ACS Appl. Mater. Interfaces*, vol. 12, no. 30, pp. 33989–33998, Jul. 2020.

[53] I. Choudhry, H. R. Khalid, and H.-K. Lee, "Flexible piezoelectric transducers for energy harvesting and sensing from human kinematics," *ACS Appl. Electron. Mater.*, vol. 2, no. 10, pp. 3346–3357, Sep. 2020.

[54] A. Arnau and D. Soares, "Fundamentals of piezoelectricity," in *Piezoelectric Transducers and Applications*, A. A. Vives, Eds. Berlin, Germany: Springer, 2009.

[55] C. Li, P.-M. Wu, S. Lee, A. Gorton, M. J. Schulz, and C. H. Ahn, "Flexible dome and bump shape piezoelectric tactile sensors using PVDF-TrFE copolymer," *J. Micromech. Syst.*, vol. 17, no. 2, pp. 334–341, Apr. 2008.

[56] S. Lee et al., "Super-flexible nanogenerator for energy harvesting from gentle wind and as an active deformation sensor," *Adv. Funct. Mater.*, vol. 23, no. 19, pp. 2445–2449, May 2013.

[57] H.-J. Tseng, W.-C. Tian, and W.-J. Wu, "Flexible PZT thin film tactile sensor for biomedical monitoring," *Sensors*, vol. 13, no. 5, pp. 5478–5492, Apr. 2013.

[58] P. Yu, W. Liu, C. Gu, X. Cheng, and X. Fu, "Flexible piezoelectric tactile sensor array for dynamic three-axis force measurement," *Sensors*, vol. 16, no. 6, p. 819, Jun. 2016.

[59] R. S. Dahiya, M. Valle, G. Metta, L. Lorenzelli, and A. Adami, "Design and fabrication of POSFET devices for tactile sensing," in *Proc. Int. Solid-State Sensors, Actuat. Microsyst. Conf.*, Jun. 2009, pp. 1881–1884.

[60] D. Y. Park et al., "Self-powered real-time arterial pulse monitoring using ultrathin epidermal piezoelectric sensors," *Adv. Mater.*, vol. 29, no. 37, Oct. 2017, Art. no. 1702308.

V. Carluccio received the M.S. degree in physics from the University of Salento, Lecce, Italy, in 2019, where she is currently pursuing the Ph.D. degree in materials and structures engineering and nanotechnologies in collaboration with the Center for Biomolecular Nanotechnologies, Istituto Italiano di Tecnologia, Lecce.

Her research interests include the realization of wearable sensors based on aluminum nitride for monitoring movements for healthcare applications.

L. Fachechi is currently a Researcher with the Center for Biomolecular Nanotechnologies, Istituto Italiano di Tecnologia, Lecce, Italy. His current research focuses on sensors powered by vibrational harvested energy by means of piezoelectric transducers and on the development of an electronic front end for piezoelectric sensors. He has long expertise in electronic hardware design and firmware implementation, as well as wireless sensor networks.

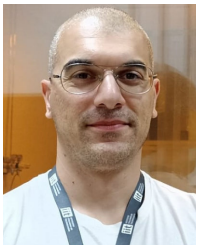

V. M. Mastronardi received the M.S. degree in ingegneria delle telecomunicazioni from the Università del Salento, Lecce, Italy, in 2012, the Ph.D. degree carrying out the Doctoral Program in Material Science and Technology from the Center for Biomolecular Nanotechnologies (CBN), Istituto Italiano di Tecnologia (IIT), Lecce, and the High Qualified Research Doctor degree in nanotechnologies and nanostructured innovative materials from the Scuola Interpolitecnica di Dottorato, Turin, Italy, in 2016.

From 2016 to 2021, he held a postdoctoral position at the CBN-IIT, working on implantable sensors based on aluminum nitride for monitoring heart activity, swallowing for early detection of dysphagia disease, and smart patches for monitoring vital parameters and sleep of astronauts. Since 2022, he has been a Researcher with the Department of Innovation Engineering, Università del Salento, working on the design and testing of wearable sensors based on piezoresistive and piezoelectric materials and inertial sensors for monitoring human physiological parameters and joint movements. Moreover, his research interests include flexible microelectromechanical systems (MEMSs), pressure and force sensors, and piezoelectric energy harvester devices.

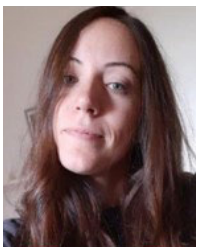

L. Natta received the M.S. degree in biomedical engineering from the Politecnico of Turin, Italy, in 2014, and the Ph.D. degree in materials and structures engineering and nanotechnology from the Università del Salento, Lecce, Italy, in collaboration with the Center for Biomolecular Nanotechnologies (CBN), Istituto Italiano di Tecnologia (IIT), Lecce, in 2019, working on flexible wearable sensors for the monitoring of physiological parameters.

Since 2019, she has been holding a postdoctoral position at CBN-IIT, focusing on the design and characterization of flexible piezoelectric sensors based on aluminum nitride.

L. Algieri received the M.S. degree in chemistry from the Università della Calabria, Arcavacata, Italy, in 2012, and the Ph.D. degree in materials and structures engineering and nanotechnology from the Università del Salento, Lecce, Italy, in collaboration with the Center for Biomolecular Nanotechnologies (CBN), Istituto Italiano di Tecnologia (IIT), Lecce, in 2018, working on the development of microelectromechanical system (MEMS) technologies based on aluminum nitride for energy harvesting.

From 2018 to 2020, she worked at PiezoSkin startup, Lecce, developing the whole fabrication protocol for soft piezoelectric transducers, characterization, and testing. Since 2020, she has been holding a postdoctoral position at the CBN-IIT, studying the contribution of microcontact parameters on friction properties for rough, piezoelectric, and electroactive surfaces.

G. de Marzo received the M.S. degree in nanobiotechnology from the University of Trieste, Trieste, Italy, in 2018, and the Ph.D. degree in materials and structures engineering and nanotechnology from the Università del Salento, Lecce, Italy, in collaboration with the Center for Biomolecular Nanotechnologies (CBN), Istituto Italiano di Tecnologia (IIT), Lecce, in 2022.

She is currently enrolled as a Postdoctoral Fellow at CBN-IIT. Her research interests include the realization of flexible and wearable sensors for physiological strains and ultrasound based on a piezoelectric biopolymer.

F. Rizzi received the Ph.D. degree in physics from the University of Bari "Aldo Moro", Bari, Italy, in 2004.

He held postdoctoral training at the Department of Physics, Institute of Photonics, University of Strathclyde, Glasgow, U.K., where he won an Experienced Researcher Marie Curie Fellowship. He is currently a Research Staff Member with the Center of Biomolecular Nanotechnologies, Istituto Italiano di Tecnologia, Lecce, Italy. He has authored more than 70 manuscripts in international journals and proceedings of international conferences, two patents, and three book chapters. His research interests and activities are related to bioinspired microelectromechanical systems' design and fabrication for applications in biological and environmental sensing, and artificial hair cells' fabrication for flow sensing in robotics.

M. De Vittorio (Senior Member, IEEE) is the Coordinator of the Center for Biomolecular Nanotechnologies, Istituto Italiano di Tecnologia, Lecce, Italy, and a Full Professor with the Università del Salento, Lecce, where he is a Lecturer of the courses "Electronic and Photonic Devices" and "Nanotechnologies for Electronics." He has been responsible for more than ten years of the Nanodevice Division at the National Nanotechnology Laboratory (NNL), CNR Istituto Nanoscience, Lecce. During his career, he has designed and coordinated microfabrication and nanofabrication facilities with both back- and front-end technologies, with full prototyping and small-/medium-scale production capabilities. He has been a consultant for high-tech corporations and a founder/advisor of four startup companies. He is the author of 280 manuscripts in indexed journals, 70 conference proceedings, 14 patents, ten book chapters, and more than 60 invited/keynote talks at international conferences. His research activity deals with the development of science and technology applied to nanophotonics, nanoelectronics, and nanoelectromechanical and microelectromechanical systems (NEMS/MEMS) for applications in the fields of life science, energy, and information and communication technology (ICT).

Dr. De Vittorio is also a Senior Editor of the IEEE TRANSACTIONS ON NANOTECHNOLOGY, a Board Member of the International Micro and Nanoengineering Society (iMNEs), and a member of the Editorial Board of the journal *Microelectronic Engineering*.

Open Access funding provided by 'Università del Salento' within the CRUI CARE Agreement